Pergamon

Bioorganic & Medicinal Chemistry 9 (2001) 151–161

BIOORGANIC & MEDICINAL CHEMISTRY

Triarylpyrazoles with Basic Side Chains: Development of Pyrazole-Based Estrogen Receptor Antagonists

Shaun R. Stauffer,[a] Ying R. Huang,[a] Zachary D. Aron,[a] Christopher J. Coletta,[a] Jun Sun,[b] Benita S. Katzenellenbogen[b,c] and John A. Katzenellenbogen[a,*]

[a]*Department of Chemistry, University of Illinois and University of Illinois College of Medicine, Urbana, IL 61801, USA*
[b]*Department of Physiology, University of Illinois and University of Illinois College of Medicine, Urbana, IL 61801, USA*
[c]*Department of Cell and Structural Biology, University of Illinois and University of Illinois College of Medicine, Urbana, IL 61801, USA*

Received 16 June 2000; accepted 15 August 2000

Abstract—Recently, we developed a novel triaryl-substituted pyrazole ligand system that has high affinity for the estrogen receptor (ER) (Fink, B. E.; Mortenson, D. S.; Stauffer, S. R.; Aron, Z. D.; Katzenellenbogen, J. A. *Chem. Biol.* **1999**, *6*, 205). Subsequent work has shown that some analogues in this series are very selective for the ERα subtype in terms of binding affinity and agonist potency (Stauffer, S. R.; Coletta, C. J.; Tedesco, R.; Sun, J.; Katzenellenbogen, J. A. *J. Med. Chem.* **2000**, submitted). We now investigate how this pyrazole ER agonist system might be converted into an antagonist or a selective estrogen receptor modifier (SERM) by incorporating a basic or polar side chain like those typically found in antiestrogens and known to be essential determinants of their mixed agonist/antagonist character. We selected an *N*-piperidinyl-ethyl chain as a first attempt, and introduced it at the four possible sites of substitution on the pyrazole core structure to determine the orientation that the pyrazole might adopt in the ER ligand binding pocket. Of these four, the C(5) piperidinyl-ethoxy-substituted pyrazole **5** had by far the highest affinity. Also, it bound to the ER subtype alpha (ERα) with 20-fold higher affinity than to ERβ. In cell-based transcription assays, pyrazole **5** was an antagonist on both ERα and ERβ, and it was also more potent on ERα. Based on structure-binding affinity relationships and on molecular modeling studies of these pyrazoles in a crystal structure of the ERα–raloxifene complex, we propose that pyrazoles having a basic substituent on the C(5) phenyl group adopt a binding mode that is different from that of the pyrazole agonists that lack this group. The most favorable orientation appears to be one which places the N(1) phenol in the A-ring binding pocket so that the basic side chain can adopt an orientation similar to that of the basic side chain of raloxifene.

Introduction

The term SERM, or selective estrogen receptor modifier, is used to describe ligands for the estrogen receptor (ER) that display an interesting balance of agonist and antagonist activity that can vary from tissue to tissue.[1] SERMs have particular utility in menopausal hormone replacement and in the treatment and prevention of breast cancer, although the pharmacological profiles of the currently available agents are not optimal.

SERMs typically consist of a non-steroidal core structure onto which is attached a side chain bearing a basic or polar function. X-ray crystal structures of the ER ligand binding domain (LBD) complexed with the SERMs raloxifene[2] or hydroxytamoxifen[3] show that the large side chains of these ligands displace the C-terminal helix (helix-12) from the position it normally occupies in ER-LBD complexes with agonists. In this antagonist conformation, helix-12 moves into a position where it occludes a hydrophobic groove on the surface of the receptor that normally functions as a tethering site for the interaction of ER with coactivator proteins, an interaction that is important in mediating agonist activity.[3,4]

It is clear, however, that more subtle changes in the conformation of ER must underlie some of the pharmacological differences among various SERMs.[5,6] Recently, conformation-sensitive peptides have been used to discriminate among these different ligand-induced ER conformations.[7–9] Nevertheless, it is not completely clear how the ligand structure of the various SERMs determines ER conformation, at least at this level of detail. In addition, differential interaction of SERMs with the two ER subtypes, ERα and ERβ, might also underlie certain aspects of their tissue-selective activity.[10–12]

*Corresponding author at Department of Chemistry, University of Illinois, 600 South Mathews Avenue, Urbana, IL 61801, USA. Tel.: +1-217-333-6310; fax: +1-217-333-7325; e-mail: jkatzene@uiuc.edu

0968-0896/01/$ - see front matter
PII: S0968-0896(00)00226-1

In recent studies of novel, heterocyclic non-steroidal estrogens amenable to combinatorial assembly and library synthesis, we identified tetrasubstituted pyrazoles as a system that afforded high affinity ligands for ER.[13] Subsequently, we used parallel synthesis, as well as directed synthesis, to characterize structure–affinity relationships in this series.[14,15] In the process, we found several high affinity compounds, and in particular, some that show very high binding affinity and transcriptional efficacy for the ER alpha subtype (ERα).[15] Although some of these compounds were also agonists on the ER beta subtype (ERβ), their potency and binding affinity on this ER subtype was much lower.[15] The high difference in ER-subtype binding affinities shown by some of these pyrazoles raised an interesting prospect that this system might be a favorable starting point for the development of ERα potency-selective antagonists or SERMs. This would depend, of course, on whether these ligands could be converted to antagonists by appropriate substitution of basic or polar side chains.

In this report, we describe the preparation of several analogues of an ERα high-affinity pyrazole which embody the type of basic or polar side chain that is typically found in SERMs. We evaluate how this substitution is tolerated in terms of ER binding affinity, and in some selected cases, we show it affects the transcriptional efficacy and potency of these ligands. We also develop a model for how these basic side chain-substituted pyrazoles are likely to be orientated in the ligand-binding pocket of ER.

Results and Discussion

An example of a favorable pattern of substitution for high affinity ER pyrazoles ligands consists of three phenols at the 1-, 3- and 5-positions and an alkyl group at the 4-position, and is shown in Figure 1 (pyrazole **1**).[13–16] The piperidinyl-ethyl substituent, which is widely represented in many SERM classes (see, for example, Raloxifene, Figure 1),[1,17] was chosen in this study as a typical basic side chain that might be expected to confer the characteristic mixed agonist/antagonist activity of these compounds. The question at hand, however, is at which position on a pyrazole such as **1** should this basic substituent be attached. Molecular modeling studies using the LBD crystal structures provided a starting point towards answering this question.

From published crystal structures, it is known that the ER-LBD adopts a different conformation when complexed with agonists (E_2, DES) versus antagonists (hydroxytamoxifen, raloxifene).[2,3] In our initial molecular modeling studies, we examined various binding modes for the pyrazole core structure (i.e. without a basic side chain) based on the larger ligand binding pocket in the ER-LBD–raloxifene (antagonist) complex.[13] However, in a subsequent publication,[15] knowing now that these pyrazoles were agonists, we reexamined our initial predictions, this time using the ER-LBD–DES (agonist) structure. As a result of this additional modeling work, as well as further structure–activity relationship studies we have done in this series of compounds,[15] we now believe that these core

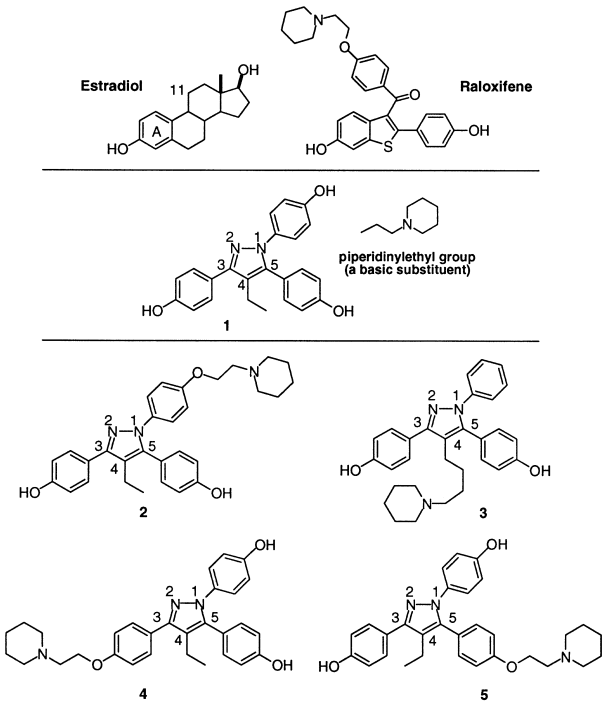

Figure 1. Pyrazole triol core structure (**1**) and basic side chain-containing pyrazoles (**2**–**5**).

pyrazoles, which behave as agonists, bind in an orientation in which the C(3) phenol plays a role analogous to the critical A-ring of estradiol.[15] We have illustrated this binding orientation with the relative positions we have chosen for pyrazole **1** and estradiol in Figure 1. The orientation of the SERM raloxifene relative to estradiol, known from X-ray crystallography,[2] is also displayed in Figure 1. In this orientation, the benzothiophene ring system of raloxifene mimics the AB ring system of estradiol, so that the basic side chain is directed roughly in the estradiol 11β direction (Fig. 1), where it extends outward to displace helix-12, as noted above.[2]

On the basis of our current model, we might have considered it unlikely that the pyrazole ligand could even accommodate a basic side chain. When bound with the ER-LBD in the agonist conformation, there is no position on the pyrazole analogue where such a side chain could be disposed so as to occupy a region of the ligand binding pocket that is normally occupied by this group in other SERMs (i.e. the estradiol 11β region, Figure 1).[2,3] However, because of the near symmetry of these triaryl pyrazoles and the known flexibility of the ligand-binding pocket of the ER,[2,3] we were not convinced that the binding orientation preferences of the smaller core pyrazole agonist ligands would be retained. The additional bulk and polarity of the basic side chain that we were adding to engender antagonist activity might cause the ligand to adopt an entirely different orientation in the binding pocket.

Therefore, as an initial effort to develop pyrazole-based SERMs, we prepared four pyrazoles in which the basic piperidinyl-ethyl side chain is attached at four different positions (**2**–**5**, Fig. 1), and we determined the binding affinity of these derivatives for the ER. Each of these

isomers serves as a model to determine which position on the heterocycle scaffold can best accommodate the SERM-defining basic side chain in the ER-LBD. Once identified, such a site would obviously be a prime target for further study through a series of pyrazoles in which the structure of this basic substituent is varied.[18]

The four basic side chain-containing pyrazoles (**2**–**5**) shown in Figure 1 are designed to probe several potential ligand orientations within the binding pocket. For example, pyrazole **2** was proposed on the basis of our initial docking study of the *N*-aryl pyrazole **1** in the ERα–raloxifene X-ray crystal structure[13] (now revised, as noted above[15]), which placed the C(5) phenol in the subpocket corresponding to the A-ring of E_2. In this mode, the N(1) basic side chain group resides in what would be the estradiol 11β direction. Pyrazole **3** was envisioned to undergo a ligand "flipping" around the bond between the pyrazole core and the C(3) phenol, to place the C(4)-linked basic side chain in the estradiol 11β direction. Pyrazoles **4** and **5** are regioisomers that have the basic side chain at the 3- and 5-positions, respectively. Pyrazole **5**, a C(5)-substituted analogue, was predicted to have a potentially favorable interaction with ER by way of a ca. 120° counterclockwise rotation about an axis perpendicular to the pyrazole ring, resulting in a binding mode that would make the N(1) phenol the mimic of the A-ring in estradiol. Pyrazole **4**, a regioisomer of pyrazole **5**, was considered unlikely to have a favorable interaction with the ER, because the phenols and the basic side chain groups are displayed in a "long" orientation. This leaves the remaining two free phenols too close to one another for proper interaction with the A-ring and D-ring subpockets in ER. Nevertheless, it was prepared for the sake of completeness.

Chemical syntheses

The synthesis of pyrazole **2** is shown in Scheme 1. For the preparation of the required piperidinyl-ethoxy-substituted phenylhydrazine, we initially investigated the classical diazotization–reduction route, starting from the corresponding substituted aniline **6**. However, we had difficulty isolating the desired hydrazine precursor. Fortunately, we found the approach of Demers and Klaubert,[19] involving metallation of the corresponding aromatic bromide (**7**) followed by reaction with an azodicarboxylate ester, conveniently afforded the di-Boc protected hydrazine **8**. Because isolation of the free hydrazine proved to be problematic, we performed the Boc deprotection and pyrazole cyclization in one-pot, which gave pyrazole **9** in 65% yield. Selective demethylation using either $AlCl_3$–EtSH or BBr_3 afforded pyrazole **2** in 55–75% yield.

The synthesis of the C(4) basic side chain-containing pyrazole **3** is shown in Scheme 2. Introduction of a basic side chain into the pyrazole structure at the 4-position was done early in the synthesis, starting with Freidel–Crafts acylation of anisole with 6-bromohexanoyl chloride. For this transformation, the temperature had to be carefully maintained at −10 °C to avoid reaction of the product ketone **10** with a second equivalent of anisole, a side reaction that results in the formation of a 1,1-diaryl-alkene by-product upon dehydration. The bromoketone **10** was then aminated with excess piperidine in DMF to afford amino-ketone **11** in high yield. Condensation with the *p*-nitrophenyl benzoate furnished the β-diketone **12**, which was cyclized with phenyl hydrazine hydrochloride to give the desired protected pyrazole **13**. Deprotection using $AlCl_3$–EtSH yielded the final pyrazole **3**.

The final pyrazoles **4** and **5** were initially prepared as an approx. 1:1 mixture of regioisomers by the route shown in Scheme 3. Starting from 4-hydroxybutyrophenone, we used a Mitsunobu reaction to prepare the piperidinyl-ethoxy-substituted ketone **14**. Claisen condensation afforded the requisite β-diketone **15**. Treatment with phenylhydrazine hydrochloride followed by BBr_3 deprotection afforded the desired pyrazoles **4** and **5** as a

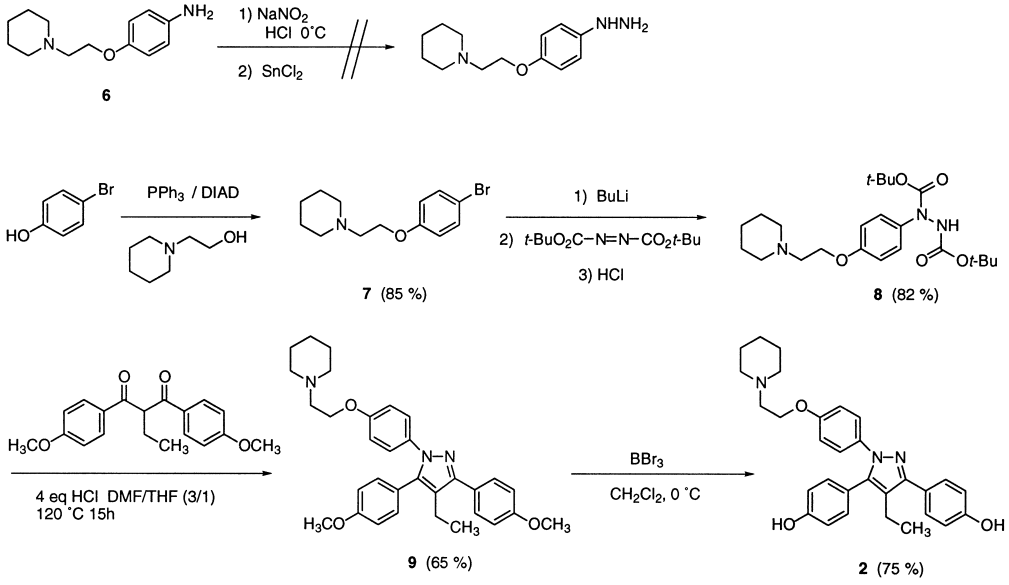

Scheme 1. Synthesis of N(1) basic side chain-containing pyrazole **2.**

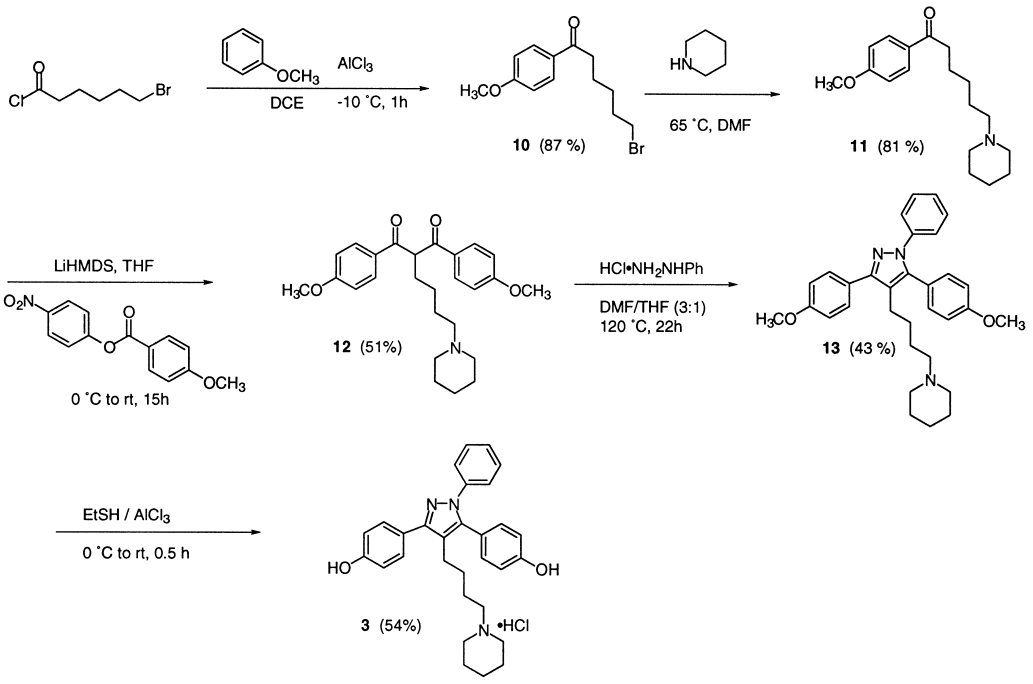

Scheme 2. Synthesis of C(4) basic side chain-containing pyrazole **3.**

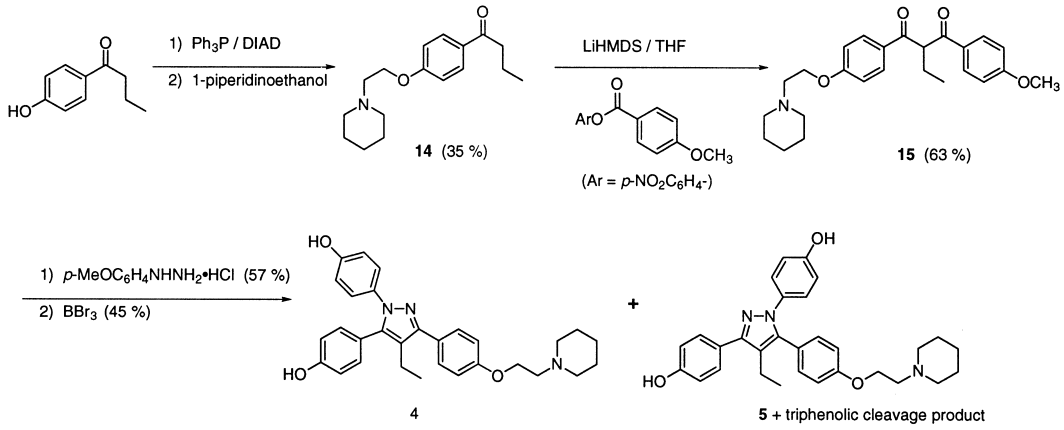

Scheme 3. Synthesis of C(3) and C(5) basic side chain-containing pyrazoles **4** and **5.**

1:1 mixture that could be separated by chromatography. Pyrazole **4** was further purified by recrystallization from MeOH, and definitive regiochemical assignment of this isomer was made on the basis of a single crystal X-ray analysis. An ORTEP diagram of this compound is shown in Figure 2.

Isolation of the last pyrazole (**5**) proved to be more problematical because we found that the basic side chain of these pyrazoles undergoes partial cleavage when BBr_3 is used as a deprotection reagent. This is a significant problem, because the triphenolic by-product resulting from this cleavage was difficult to separate from the desired C(5) basic side chain isomer by chromatography and it has distinctly different biological activity.[15] Later, we found that we could do this deprotection selectively, without this side reaction, using the milder $AlCl_3$–EtSH reagent. Ultimately, however, we used a regioselective route (described elsewhere in detail[18]) to produce the desired pyrazole **5**.

Estrogen receptor binding affinity of pyrazoles 2–5

The binding affinity of pyrazoles **2**–**5** for ER was assayed in a competitive radiometric binding assay as described previously,[20,21] and affinities are expressed as relative binding affinity (RBA) values, where the affinity of estradiol is considered to be 100% (Table 1). The affinity of all compounds was tested both in a natural ER preparation from lamb uterine cytosol,[21] which is predominantly ERα,[10,11] as well as with purified recombinant human ERα and ERβ (see Experimental).[20]

When uterine cytosol was used as a source of estrogen receptor, pyrazole **2** had a relatively low binding affinity, just 1.5% that of estradiol, a value which is 10-fold lower than that of the parent N(1) aryl pyrazole (**1**).[13,15] Pyrazole **3** with the basic side chain on C(4) also displayed very low affinity for the receptor. Apparently, even with the reorientation proposed above, this analogue, in which the basic side chain is attached to the pyrazole

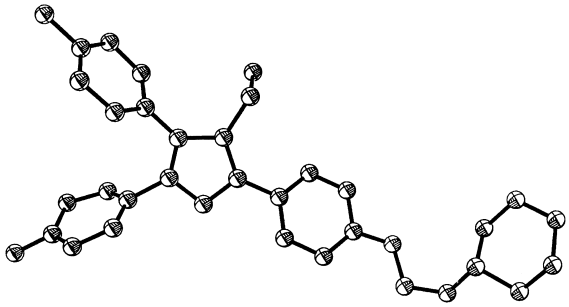

Figure 2. X-ray crystal structure for **4** (ORTEP; ellipsoids drawn at the 35% probability level).

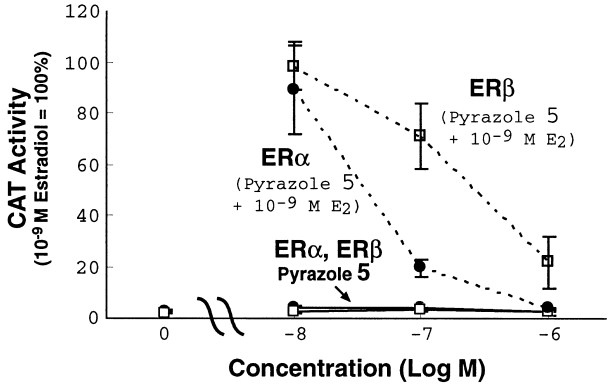

Figure 3. Transcription activation profile for pyrazole **5** with ERα and ERβ. Human endometrial cancer (HEC-1) cells were transfected with expression vectors for ERα or ERβ and an $(ERE)_3$-pS2-CAT reporter gene and were treated with indicated concentrations of pyrazole **5** alone (solid lines) or pyrazole **5** in the presence of 10^{-9} M estradiol (E_2) (dashed lines) for 24 h. CAT activity was normalized for β-galactosidase activity from an internal control plasmid. Values are the mean ±SD for three separate experiments, and are expressed as a percent of the ERα or ERβ response with 10^{-9} M E_2, which is set at 100%. For some values, error bars are too small to be visible.

core solely through aliphatic linkages, does not fit well in the ligand binding pocket of ER. More intriguing are the two regioisomeric pyrazoles **4** and **5**; they display very distinctive preferences for binding to the ER, pyrazole **5** having a 65- to 90-fold higher affinity than pyrazole **4** in all three test systems. As noted previously, the higher affinity of isomer **5** versus **4** was expected.

Pyrazole **5** has the highest affinity of all basic side chain pyrazoles investigated thus far, and, in fact, is among the highest affinity of all pyrazoles we have reported as ER ligands.[13–15] When we evaluated the binding affinity of these pyrazoles with pure human ERα and ERβ (Table 1),[20] pyrazole **5** showed a distinctive preference for binding to ERα (ca. 20-fold), a characteristic that it shares with the parent pyrazole triol **1** (ca. 230-fold).[15] Pyrazole **2** shows only a 5-fold affinity preference for ERα. Pyrazoles **3** and **4** had very low affinity for both ERα and ERβ, and they were not investigated further either for binding affinity or transcriptional activity.

Transcription activity of pyrazole 5

Based on the promising ERα binding selectivity of pyrazole **5** and because of its piperidine side chain, we were interested in whether this compound had antagonistic properties, and in particular, whether it might function as an antagonist on one or both of the ER subtypes in a potency selective manner. Figure 3 shows the transcriptional activity profiles of pyrazole **5** assayed in HEC-1 cells with either ERα or ERβ. Cells were transfected with an expression plasmid for ERα or ERβ, together with an estrogen-responsive reporter gene construct ($(ERE)_3$-pS2-CAT), and reporter gene expression was determined at different concentrations of ligand. Antagonism was assayed at different concentrations of ligand in the presence of 10^{-9} M E_2.

Table 1. Estrogen receptor binding affinity of pyrazoles **1–5**

Compound	Site of basic side chain	RBA lamb uterine cytosol[a]	RBA hERα[a]	RBA hERβ[a]
1	[none]	20.3±3	35.7±6	0.15±0.01
2	N(1)	1.5±0.4	0.65±0.13	0.13±0.03
3	C(4)	0.017±0.006	0.05[b]	0.019[b]
4	C(3)	0.29±0.26	0.13[b]	0.01[b]
5	C(5)	24.5±1	11.5±1	0.65±0.02

[a]Relative binding affinity (RBA) where estradiol = 100%. Values are the average of repeat determinations±SD ($n \geq 3$) or ±range ($n = 2$). For details of the assay procedure, see Experimental.
[b]Single determinations.

Pyrazole **5** showed no stimulation of transcriptional activity of ERα or ERβ, and it was a full antagonist on ERα and ERβ, completely antagonizing activity stimulated by estradiol (Fig. 3). Thus, introduction of the type of basic side chain typically found in the mixed agonist/antagonist SERMs at the proper site on the parent pyrazole **1**, which is an agonist, converts this pyrazole system into an antagonist (pyrazole **5**). The relatively good ERα binding affinity selectivity of pyrazole **5** (ca. 20-fold; cf. Table 1) is preserved to a considerable degree in its potency as a transcriptional antagonist. Its IC_{50} value is ca. 20 nM on ERα and ca. 160 nM on ERβ, which gives an ERα antagonist potency selectivity of ca. 10-fold (Fig. 3).

In work to be presented elsewhere, we have prepared additional analogues of pyrazole **5** having other basic and polar side chains as substituents on the C(5) phenyl group.[18] Some of these have very high affinity selectivity for ERα over ERβ, and they act as ERα potency selective antagonists (J. Sun et al., in preparation).

Binding models for pyrazoles 2 and 5 in the ERα–raloxifene crystal structure

As previously mentioned, the low binding affinity of pyrazole **4** was not surprising. The low affinity of pyrazole **3**, however, was unexpected, because, as mentioned earlier, when the pyrazole core is flipped, the basic side chain attached to C(4) appears to be orientated properly for this substituent to project through the 11β channel.

Pyrazole **2**, in which the basic side chain is substituted on the N(1) phenyl group, was initially believed to be the most favorable candidate for interacting with ER. However, this turned out not to be the case; pyrazole **5** has the

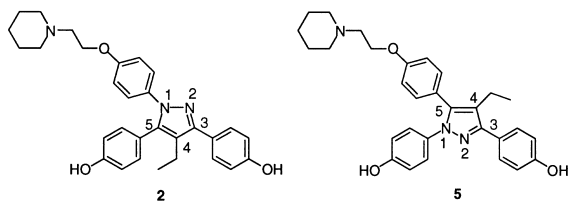

Figure 4. Pyrazoles **2** and **5** oriented with corresponding aryl rings oriented in a congruent fashion.

highest affinity. These two pyrazoles have somewhat related structures (cf. Fig. 1); the three aryl groups (two unsubstituted and one side chain-substituted) can be superimposed in a congruent fashion, as illustrated in Figure 4. When oriented in this fashion, the only difference between these two isomers is the position of the two ring nitrogen atoms and the C(4) ethyl substituent.

In an attempt to understand the 16-fold higher affinity of pyrazole **5** than pyrazole **2**, we performed some docking studies of these two ligands with the ERα–raloxifene crystal structure.[2] Both ligands were docked in the ERα–raloxifene crystal structure in a similar manner, and they were subjected to a three-step minimization protocol to generate the final receptor–ligand model complexes shown (see Experimental, Molecular Modeling for details). Residue side chains that were close to each ligand in its initial position were allowed to undergo torsional movement during the docking operation, in order to obtain an optimal fit, prior to minimization. A crossed-stereo view of pyrazoles **2** and **5** is shown in Figure 5(A) and (B). The final models have similar energies, which at least at this level of refinement, simply indicates that they have no bad contacts or unfavorable conformations.

In both of the views shown in Figure 5, the three aryl groups displayed peripherally from the pyrazole core are accommodated comfortably and in a very similar manner within the ligand binding pocket. This was achieved with only minimal and energetically favorable movement of a few residues that were initially in close contact with the ligand.

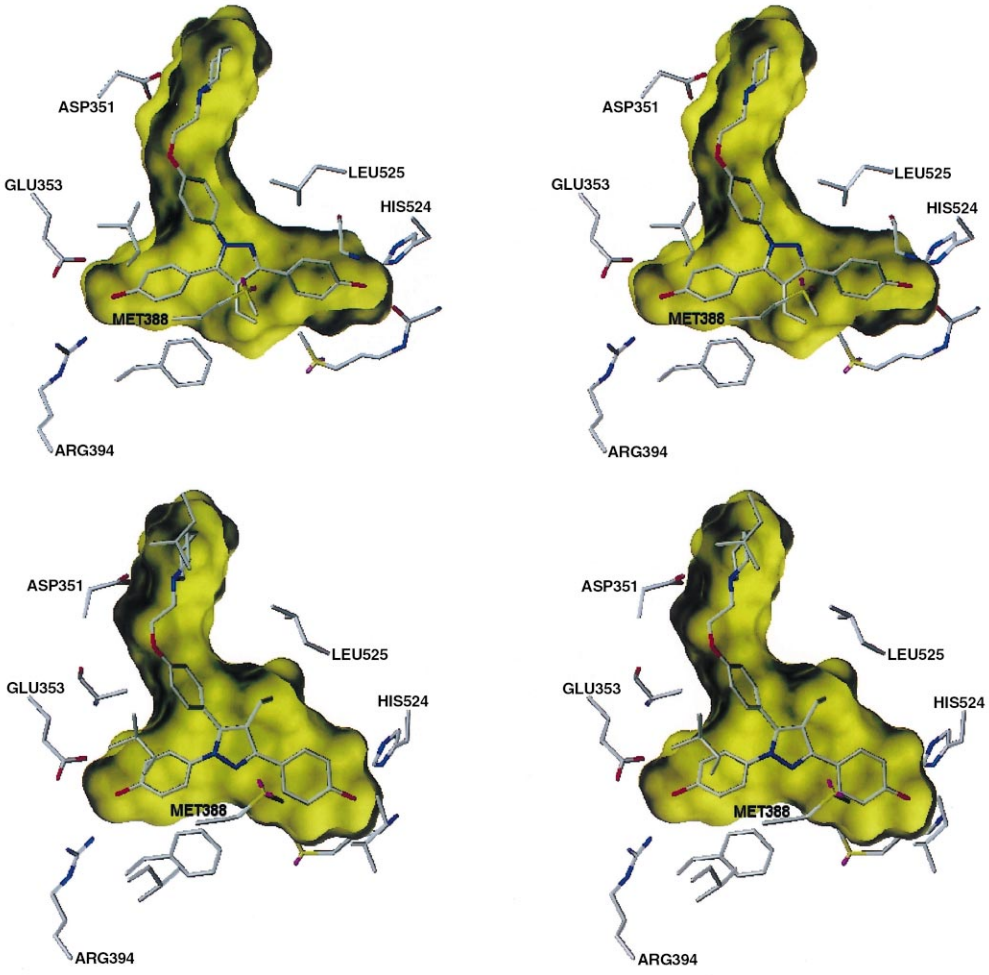

Figure 5. Crossed-stereo views of pyrazole **2** (top) and **5** (bottom) docked and minimized in ERα–raloxifene structure ligand binding pocket showing residues within 2.5 Å of ligand. The pyrazoles were initially positioned with respect to certain reference atoms of the ligand raloxifene, and then minimized together with the same contact residues in the protein using the Flexidock routine within SYBYL. For details, see Experimental. The yellow surface is a cutaway of the Connolly surface of the protein ligand-binding pocket.

The most significant difference between the complexes with pyrazoles **2** and **5** is the position of the ethyl group (cf. Fig. 4). In Figure 5(B), the C(4) ethyl group of pyrazole **5** projects into a region of ER that accommodates the 18-methyl of estradiol in the ER–E_2 complex.[2] In this subpocket, the favorable van der Waals interaction that normally occurs between Leu525 and the 18-methyl group of E_2 is conveniently replaced by a similar interaction with the ethyl substituent of pyrazole **5** (Fig. 5(B)).

By contrast, in the complex with pyrazole **2**, the ethyl substituent is oriented in a different position (downward), where it no longer benefits as much from a favorable hydrophobic–hydrophobic interaction, as was the case in the complex with pyrazole **5**. Leu525 is somewhat closer to the pyrazole core, where it interacts with the N(1) phenyl ring. The closest residue for interaction with the C(4) ethyl of pyrazole **2** (Fig. 5(A)) is Met388. This residue is a somewhat "softer" partner for interaction than Leu525, and may be less stabilizing. Other differences between the ER complexes with pyrazoles **2** and **5** which could account for their differing binding affinity may have to do with electronic effects and are not considered in these models. As noted earlier (Fig. 4), the positions of the nitrogen atoms are different between the two binding modes, so the electronic molecular surfaces that are presented to the receptor are predicted to be quite different.

Conclusions

We have prepared a series of basic side chain-substituted pyrazoles as potential selective antagonists for ER subtypes. The initial four analogues were designed to explore the four possible orientations that the pyrazole core structure might adopt in the ER ligand binding pocket, and thereby to identify which site on the pyrazole could best accommodate the rather large, basic side chain substituent. Of the four analogues, the C(5) piperidinyl-ethoxy-substituted pyrazole **5** was found to have the highest affinity for ERα, with an affinity among the highest observed for all ER ligands of the pyrazole type. It also shows considerable affinity selectivity for ERα versus ERβ. Through cell-based transfection assays, we found that pyrazole **5** was an antagonist on both ERα and ERβ, and that its potency on ERα was somewhat higher, reflecting its ERα affinity selectivity. Modeling studies using the crystal structure of the ERα–raloxifene complex were used to compare potential binding modes for pyrazoles **2** and **5**. The binding modes appear to be quite similar, and the origin of the higher affinity for pyrazole **5** versus **2** may result from a more favorable positioning of the ethyl group in the binding pocket in the complex with pyrazole **5**. In work to be presented elsewhere, we have prepared additional analogues of pyrazole **5** having other basic and polar side chains as substituents on the C(5) phenyl group.[18] Some of these have very high affinity selectivity for ERα over ERβ, and they act as ERα potency selective antagonists (J. Sun et al., in preparation). This work is the first effort towards developing a novel SERM based on a pyrazole core structure.

Experimental

General

Melting points were determined on a Thomas-Hoover UniMelt capillary apparatus and are uncorrected. All reagents and solvents were obtained from Aldrich, Fisher or Mallinckrodt. Tetrahydrofuran was freshly distilled from sodium/benzophenone. Dimethylformamide was vacuum distilled prior to use, and stored over 4 Å molecular sieves. *n*-Butyllithium was titrated with *N*-pivaloyl-*o*-toluidine. Et_3N was stirred with phenylisocyanate, filtered, distilled, and stored over 4 Å molecular sieves. All reactions were performed under a dry N_2 atmosphere unless otherwise specified. Reaction progress was monitored by analytical thin-layer chromatography using GF silica plates purchased from Analtech. Visualization was achieved under illumination with short wave UV light (254 nm) or with a potassium permanganate indicator spray. Radial preparative-layer chromatography was performed on a Chromatotron instrument (Harrison Research, Inc., Palo Alto, CA) using EM Science silica gel Kieselgel 60 PF_{254} as adsorbent. Flash column chromatography was performed using Woelm 32–63 μm silica gel packing. The preparation of pyrazole **5** by a regioselective route is described elsewhere.[18]

^1H and ^{13}C NMR spectra were recorded on either a Varian Unity 400 or 500 MHz spectrometers using $CDCl_3$ or MeOD-d_4 as solvent. Chemical shifts were reported as parts per million downfield from an internal tetramethylsilane standard (δ 0.0 for ^1H) or relative to solvent peaks. NMR coupling constants are reported in Hertz. ^{13}C NMR spectra were determined using either the Attached Proton Test (APT) or standard ^{13}C pulse sequence parameters. Low-resolution and high-resolution electron impact mass spectra were obtained on Finnigan MAT CH-5 or 70-VSE spectrometers. Elemental analyses were performed by the Microanalytical Service Laboratory of the University of Illinois. Single crystal X-ray analysis on pyrazole **4** was performed to determine connectivity. A rigorous analysis was not performed because of the presence of a disordered solvent molecule in the unit cell. However, for the purposes of regiochemical assignment, the analysis was satisfactory.

Biological procedures

Relative binding affinity assay. Ligand binding affinities (RBAs) using lamb uterine cytosol as a receptor source were determined by a competitive radiometric binding assay using 10 nM [^3H]estradiol as tracer and dextran-coated charcoal as an adsorbent for free ligand, as previously described.[21] Binding affinities with purified recombinant human ERα and ERβ were determined by a competitive radiometric binding assay using 10 nM [^3H]estradiol as tracer, commercially available ERα and ERβ preparations (PanVera Inc. Madison, WI), and hydroxylapatite (HAP) to adsorb bound receptor–ligand complex.[20] HAP was prepared following the recommendations of Williams and Gorski.[22] All incubations were done at 0 °C for 18–24 h. Binding affinities are expressed relative to estradiol (RBA = 100%) and are reproducible with a coefficient of variation of 0.3.

Transcriptional activation assay. Human endometrial cancer (HEC-1) cells were maintained in culture and transfected as described previously.[23,24] Transfection of HEC-1 cells in 60 mm dishes used 0.4 mL of a calcium phosphate precipitate containing 0.5 μg of pCMVβGal as internal control, 2 μg of the reporter gene plasmid, 100 ng of the ER expression vector, and carrier DNA to a total of 5 μg DNA. Compounds were added to the cell culture media as ethanol solutions so as to yield a final ethanol concentration of 0.1%. CAT activity, normalized for the internal control β-galactosidase activity, was assayed as previously described.[23,24]

Molecular modeling

Small molecule modeling. The starting structures of pyrazoles **2** and **5** used for the ER-LBD docking studies were generated from random conformational searches using the TRIPOS force field as implemented in Sybyl 6.5.2. Low energy conformers then underwent full minimization until a convergence criterion of 0.001 kcal/mol was met using the AM1 semi-empirical force field. Charge calculations were done using Gasteiger–Huckel method and molecular surface properties displayed using MOLCAD module in Sybyl 6.5.2.

Receptor docking studies. The lowest energy conformers for pyrazoles **2** and **5**, generated as indicated above, were used for docking studies. Prior to docking, a +1 formal charge and a proton were added to each piperidinyl nitrogen. Ligands were then pre-positioned in the crystal structure of the ERα–raloxifene complex,[2] using a least squares multifitting of the most congruent atoms of the pyrazole and raloxifene. In raloxifene this included the A-ring carbon atoms and the 1,4-carbon atoms in both the 2- and 3-substituted phenyl groups. The same fitting strategy was used in the pyrazoles, all six carbon atoms in the ring corresponding to the A-ring and the 1,4-carbon atoms of the other two aryl rings. Once pre-positioned, the raloxifene structure was deleted and then the pyrazole ligand was optimally docked in the ERα binding pocket using the TRIPOS Flexidock routine. Hydrogen bond donors (Arg394, His524) and hydrogen bond acceptors (Glu353, His524, and Asp351) in ER were indicated in Flexidock, as well as the hydrogen bond donors and acceptors in the ligand. Side chains that were allowed to rotate during docking of the pyrazoles **2** and **5** included Met543, Leu539, Leu536, Leu354, Asp351, Trp383, all of which are near the basic side chain group; Phe404, Leu387, and Met388, which are near the A-ring mimic; Leu384, Leu346, Leu428, and Trp383, which are near the B/C ring region; and Ile424, His524, and Leu525, which are near the D-ring subpocket. Arg394 and Glu353, the hydrogen bonding partners of the critical A-ring phenol mimic, were kept fixed during the entire docking and minimization.

The best docked ligand ER-LBD complex from the Flexidock routine then underwent a three-step minimization: First, non-ring torsional bonds of the ligand were minimized in the context of the receptor, using the torsmin command. This was followed by minimization of the side chain residues within 8 Å of the ligand while holding the backbone and residues Glu353 and Arg394 fixed. A final, third minimization of both the ligand and receptor was conducted using the Anneal function (hot radius 8 Å, interesting radius 16 Å), again holding residues Glu353 and Arg394 fixed. The result of this was considered to be the final model. Minimizations were done using the TRIPOS Forcefield (MAXIMIN) with the Powell gradient method and default settings (final RMS < 0.05 kcal/mol·Å). The total energy for the ERα complex with pyrazole **2** was −806 kcal/mol and for the complex with pyrazole **5** was −868 kcal/mol. At this level of refinement, these numbers cannot be used to predict relative binding affinities. However, they indicate that there are no serious errors or unfavorable contacts in the ER-LBD ligand models.

Chemical synthesis

1-[4-(2-*N*-Piperidinyl-ethoxy)-phenyl]-3,5-di-(4-hydroxyphenyl)-4-ethyl-pyrazole (2). To a stirred solution of the protected pyrazole **9** (100 mg, 0.19 mmol) in CH_2Cl_2 (1.0 mL) at 0 °C was added BBr_3 (1.0 M CH_2Cl_2, 5 equiv, 0.95 mL) dropwise. The reaction was kept at 0 °C for 4 h and then quenched with water. The solution was neutralized with satd $NaHCO_3$ and then repeatedly extracted with EtOAc. The combined organic layers were washed with brine, dried over Na_2SO_4 and concentrated to afford a tan residue. Purification by flash chromatography (5% TEA and 5% MeOH in CH_2Cl_2) afforded **2** as an off-white powder (75%): mp 125–130 °C (decomposed); ^{1}H NMR ($CDCl_3$, 400 MHz) δ 0.98 (t, 3H, $J=7.3$), 1.51 (br s, 2H), 1.62 (quint, 4H, $J=5.5$), 2.58 (q, 2H, 7.5), 2.67 (br s, 4H), 2.89 (t, 2H, $J=5.5$), 4.13 (t, 2H, $J=5.5$), 6.76 (d, 2H, $J=8.5$), 6.87 (d, overlapping, 2H, $J=8.5$), 6.88 (d, overlapping, 2H, $J=9$), 7.03 (d, 2H, $J=8.5$), 7.16 (d, 2H, $J=9.0$), 7.49 (d, 2H, $J=8.5$); APT ^{13}C NMR ($CDCl_3$, 100 MHz) δ 9.9 (CH_3), 18.5 (CH_2), 24.8 (CH_2), 26.2 (CH_2), 54.1 (CH_2), 56.1 (CH_2), 58.8 (CH_2), 116.1 (CH), 116.8 (CH), 116.9 (CH), 121.4 (C), 123.1 (C), 126.8 (C), 128.5 (CH), 130.9 (CH), 133.0 (CH), 135.2 (C), 144.0 (C), 152.6 (C), 159.1 (C), 159.4 (C), 159.5 (C); MS (EI, 70 eV) *m*/*z* 483.3 (M); HRMS (EI) calcd for $C_{30}H_{33}N_3O_2$ (M^+-HBr): 483.2522. Found: 481.2365 ($M^+-HBr-2$).

4-(4-*N*-Piperdinyl-butyl)-3,5-di-(4-hydroxyphenyl)-1-phenylpyrazole hydrochloride (3). To a stirred CH_2Cl_2 (1.0 mL) solution of the protected pyrazole **13** (72 mg, 0.15 mmol) was added $AlCl_3$ (116 mg, 0.87 mmol). The mixture was cooled to 0 °C and EtSH (55 μL, 0.73 mmol) added dropwise. The mixture was then allowed to reach rt and stirred for an additional 0.5 h. At this time the reaction was concentrated under a stream of nitrogen in a fume hood, brought up in CH_2Cl_2 and concentrated once again. The crude mixture was re-dissolved in CH_2Cl_2 and a mixture of THF (1 mL), water (1 mL), and 6 M HCl (0.25 mL) added. The resulting precipitate was isolated by vacuum filtration and was washed with four 5 mL portions of water followed by four 5 mL portions of ether to afford pyrazole **3** as a white solid (37 mg, 54%): ^{1}H NMR (MeOD-d_4, 500 MHz) δ 1.30–1.60 (m, 6H), 1.75 (br s, 6H), 2.73 (t, 2H, $J=7.2$), 2.78

(t, 4H, $J=8.1$), 6.90 (XX′ of AA′XX′, 2H, $J_{AX}=8.8$, $J_{XX''}=2.5$), 7.07 (AA′ of AA′XX′, 2H, $J_{AX}=8.8$, $J_{AA'}=2.5$), 7.23–7.36 (m, 5H), 7.32 (XX′ of AA′XX′, 2H, $J_{AX}=8.6$, $J_{XX'}=2.4$), 7.52 (AA′ of AA′XX′, 2H, $J_{AX}=8.6$, $J_{AA'}=2.2$); ^{13}C NMR (MeOD-d_4, 125 MHz) δ 21.5, 22.5, 22.3, 23.0, 27.0, 52.8, 56.6, 115.1, 115.2, 117.4, 121.1, 124.8, 124.9, 127.0, 127.3, 128.5, 131.2, 139.8, 142.4, 151.5, 157.5, 157.9; MS (EI, 70 eV) *m*/*z* (relative intensity, %): 467 (M^+-HCl, 21); HRMS (EI, M^+) calcd for $C_{30}H_{33}N_3O_2$: 467.2573. Found: 467.2579.

1-(4-Hydroxyphenyl)-3-[4-(2-*N*-piperidinyl-ethoxy)-phenyl]-4-ethyl-5-(4-hydroxy-phenyl)-1*H*-pyrazole (4). A CH_2Cl_2 solution (10 mL) of the crude protected pyrazole isomers (300 mg, 0.60 mmol) prepared from the 1,3-dione **15** was cooled to 0 °C and treated dropwise with BBr_3 (1 M in hexane, 5 equiv, 3 mmol). The reaction was allowed to reach temperature and stir overnight. The mixture was re-cooled to 0 °C and quenched with 5 mL of MeOH and the solvent removed under reduced pressure. To the crude mixture 8 mL of H_2O was added and the aqueous layer neutralized with a satd aqueous $NaHCO_3$ solution and extracted repeatedly with EtOAc (5×20 mL). The organic layers were washed with brine, dried over Na_2SO_4 and concentrated in vacuo to afford a brown residue. Pyrazole **4** was cleanly separated from the regioisomer **5** and other byproducts by flash chromatography (7% Et_3N and 7% MeOH in CH_2Cl_2). It was further purified by recrystallization from MeOH to afford the C(3) isomer (**4**) as small white crystals whose structure was verified by X-ray analysis (23%). Pyrazole **4**: mp 151–153 °C; ^{1}H NMR ($(CD_3)_2SO$, 400 MHz) δ 1.01 (t, 3H, $J=7.6$), 1.43 (m, 2H), 1.55 (m, 4H), 2.49 (br s, 4H), 2.59 (q, 2H, $J=7.6$), 2.72 (t, 2H, $J=5.6$), 4.15 (t, 2H, $J=6.0$), 6.74 (d, 2H, $J=8.4$), 6.83 (d, 2H, $J=8.4$), 7.08 (apparent triplet due to three overlapping doublets, 6H, $J=7.6$), 7.67 (d, 2H, $J=8.4$), 9.71 (br s, 2H, OH exchangeable with D_2O); APT ^{13}C NMR ($(CD_3)_2SO$, 100 MHz) δ 15.4 (CH_3), 16.8 (CH_2), 23.9 (CH_2), 25.6 (CH_2), 54.5 (CH_2), 57.5 (CH_2), 65.6 (CH_2), 114.5 (CH), 115.1 (CH), 115.4 (CH), 118.7 (C), 120.9 (C), 126.1 (CH), 126.5 (C), 128.5 (CH), 131.2 (CH), 131.8 (C), 141.2 (C), 148.5 (C), 156.2 (C), 157.4 (C), 157.9 (C); HRMS (EI, M^+) calcd for $C_{30}H_{33}N_3O_3$: 483.2521. Found: 483.2516.

As was noted in the text, isolation of the other regioisomer (pyrazole **5**) from this reaction mixture was complicated by the fact that it could not be separated effectively from the triphenolic byproduct that resulted from partial cleavage of the basic side chain during the BBr_3 deprotection. This compound was prepared in a regioselective fashion by another route that is described elsewhere.[18]

1-Bromo-4-(2-*N*-piperidinyl-ethoxy)benzene (7). In a 250 mL flask charged with Ph_3P (35 mmol) in 60 mL of THF at 0 °C was added di-*iso*-propyl-azodicarboxylate (DIAD, 35 mmol) reagent dropwise. The solution was kept at 0 °C and stirred for 50 min. At this time *N*-(2-hydroxyethyl)-piperidine was added dropwise via syringe. After 10 min, *p*-bromophenol (35 mmol) and TEA (86.7 mmol) in 20 mL THF were added dropwise via an addition funnel. After 1 h at 0 °C the reaction was warmed to rt and stirred for 6 h. The crude mixture was then concentrated in vacuo and the Ph_3PO byproduct removed by vacuum filtration. The filtrate was again concentrated and the product purified by gradient flash chromatography using 5% TEA and 30% EtOAc in hexanes up to 5% TEA and 50% EtOAc in hexanes to afford **7** as a clear oil (85%):[25] ^{1}H NMR ($CDCl_3$, 500 MHz) δ 1.41 (m, 2H), 1.58 (m, 4H), 2.47 (br s, 4H), 2.72 (d, 2H, $J=7.2$), 4.05 (d, 2H, $J=7.6$), 6.79 (d, 2H, 8.3), 7.82 (d, 2H, $J=8.1$); ^{13}C NMR ($CDCl_3$, 125 MHz) δ 22.1, 38.0, 67.5, 113.0, 116.5, 121.8, 123.8, 132.3, 136.6, 149.6, 158.0, 158.3; MS (EI, 70 eV) *m*/*z* 284 (M^+).

***N*,*N*-di-*tert*-Butoxycarbonyl-*N*-[4-(2-*N*-piperidinyl-ethoxy) phenyl]hydrazine (8).** To a THF solution at −70 °C containing the substituted bromobenzene **7** (10.56 mmol) was added *n*-BuLi (1.3 equiv) dropwise over 10 min. After 30 min, *tert*-butoxycarbonyl-azodicarboxylate (15.84 mmol) was added as a solid in one portion. The mixture was then slowly warmed to rt and 1 equiv of dilute AcOH added. After stirring the quenched mixture for 30 min, the reaction was partitioned between water (30 mL) and Et_2O (50 mL). The layers were separated and the aqueous layer extracted twice more with Et_2O (2×50 mL). The combined organic layers were washed with brine and dried over Na_2SO_4. Subsequent solvent removal afforded 6.8 g of a crude red oil. Flash chromatography (5% TEA and 25% EtOAc in hexanes) produced **8** as a white solid (75%): mp 50–55 °C; (note: spectrum complicated by Boc rotamers); ^{1}H NMR ($CDCl_3$, 400 MHz) δ 1.38 (s, 9H), 1.40 (overlapping s, 11H), 1.61 (m, 4H), 2.45 (m, 4H), 2.73 (t, 2H, $J=5.6$), 4.05 (t, 2H, $J=5.3$), 6.82 (d, 2H, $J=7.8$), 7.25 (br s, 2H); ^{13}C NMR ($CDCl_3$, 100 MHz) δ 24.2 (CH_2), 24.8 (CH_2), 28.2 (CH_3), 28.3 (CH_3), 36.8 (CH_2), 46.0 (CH_2), 46.7 (CH_2), 55.1 (CH_2), 57.8 (CH_2), 60.4 (CH_2), 65.7 (CH_2), 66.0 (CH_2), 81.0 (CH_2), 81.8 (CH_2), 113.9 (CH), 114.6 (CH), 120.7 (CH), 129.4 (CH), 156.7 (C), 158.7 (C), 171.2 (C); MS (EI, 70 eV) *m*/*z* 435.4 (M, 35%). Anal. ($C_{23}H_{37}N_3O_5$): C, 63.42; H, 8.56; N, 9.65. Found: C, 63.20; H, 8.72; N, 9.47.

1-[4-(2-*N*-Piperidinyl-ethoxy)-phenyl]-3,5-bis-(4-methoxy-phenyl)-4-ethyl-1*H*-pyrazole (9). To a stirred solution of DMF (14 mL), THF (6 mL), and 1,3-bis-(4-methoxy-phenyl)-2-ethyl-propane-1,3-dione (500 mg, 1.52 mmol)[15] was added hydrazine **8** in 3-fold excess (800 mg, 4.59 mmol). The mixture was brought to reflux for 5 h and then recooled to rt. The THF was removed under reduced pressure and the remaining residue diluted with H_2O (30 mL) and extracted repeatedly with EtOAc. The organic layers were washed with brine, dried over Na_2SO_4 and concentrated to produce a crude red–orange oil. Flash chromatography using 10% TEA and 20% EtOAc in hexanes afforded the pure product **9** as an orange oil (65%): ^{1}H NMR ($CDCl_3$, 400 MHz) δ 1.03 (t, 3H, $J=8.1$), 1.42 (m, 2H), 1.58 (quin, 4H, $J=6$); 2.47 (br s, 2H), 2.61 (q, 2H, $J=6.2$), 2.72 (t, 2H, $J=6$), 3.79 (s, 3H), 3.82 (s, 3H), 4.04 (t, 2H, $J=6.2$), 6.76 (d, 2H, $J=9.0$), 6.86 (d, 2H, $J=9.0$), 6.96 (d, 2H, $J=9.1$), 7.13 (d, 2H, $J=9.1$), 7.16 (d, 2H, $J=9.1$), 7.69 (d, 2H, $J=9.0$); ^{13}C NMR ($CDCl_3$, 100 MHz) δ 15.6 (CH_3),

17.2 (CH_2), 24.3 (CH_2), 26.0 (CH_2), 55.1 (CH_3), 55.2 (CH_3), 57.9 (CH_2), 66.2 (CH_2), 113.8 (CH), 113.9 (CH), 114.5 (CH), 119.9 (C), 123.3 (C), 126.0 (CH), 126.9 (C), 129.0 (CH), 131.3 (CH), 133.6 (C), 141.0 (C), 150.1 (C), 157.4 (C), 159.1 (C), 159.4 (C); HRMS (EI, M^+) calcd for $C_{32}H_{37}N_3O_2$: 511.2834. Found: 511.2825.

6-Bromo-1-(4-methoxy-phenyl)-hexan-1-one (10). To a stirred solution of $AlCl_3$ (12.40 g, 92.75 mmol) in 1,2-dichloroethane (30 mL) at 0 °C was added 6-bromohexanoyl chloride (23.70 g, 17 mL, 111.30 mmol) dropwise over 10 min. The resulting solution was stirred at rt for 0.5 h, cooled to −15 °C and a solution of anisole (10.00 g, 10.05 mL, 92.75 mmol) in 1,2-dichloroethane (10 mL) was added dropwise over 20 min. The reaction mixture was allowed to stir at −15 °C for 1 h, then quenched with H_2O (50 mL). The aqueous layer was isolated and extracted with CH_2Cl_2 (2×50 mL), and the organic layers were combined and washed with H_2O (2×50 mL), saturated $NaHCO_3$ (2×50 mL), and brine (2×50 mL). Subsequent drying over Na_2SO_4 and solvent removal in vacuo afforded a crude orange oil. Upon standing at rt, large crystals formed after 48 h. The crystals were isolated and rinsed with cold hexane to afford **10** (23 g, 87%): mp 50–52 °C; ^1H NMR ($CDCl_3$, 400 MHz) δ 1.52 (quint, 2H, $J=7.6$), 1.76 (quint, 2H, $J=7.5$), 1.91 (quint, 2H, $J=7.1$), 2.94 (t, 2H, $J=7.3$), 3.42 (t, 2H, $J=6.7$), 3.87 (s, 3H), 6.93 (d, 2H, $J=8.8$), 7.94 (d, 2H, $J=9.0$); ^{13}C NMR ($CDCl_3$, 100 MHz) δ 23.39, 27.79, 32.51, 33.59, 37.80, 55.34, 113.56, 129.88, 130.13, 163.24, 198.48; HRMS (EI, M^+) calcd for $C_{13}H_{17}O_2Br$: 286.0391. Found: 286.0394.

1-(4-Methoxy-phenyl)-6-(*N*-piperidinyl)-hexan-1-one (11). To a stirred solution of ketone **10** (248 mg, 1.00 mmol) in DMF (30 mL) at 0 °C was added piperidine (170 mg, 0.20 mL, 2.00 mmol) dropwise over 5 min. The solution was placed in a 70 °C oil bath for 4 h and then cooled to rt. The crude mixture was concentrated under reduced pressure to remove a majority of the DMF and excess piperidine to afford an orange residue. The residue was taken up in CH_2Cl_2 (30 mL), washed with brine (2×20 mL), dried over $MgSO_4$ and concentrated under reduced pressure to afford **11** as a white solid (227 mg, 79%): mp 163–165 °C; ^1H NMR ($CDCl_3$, 500 MHz) δ 1.35–1.45 (m, 2H), 1.65–2.00 (m, 8H), 2.26 (br q, 2H, $J=8$), 2.59 (br q, 2H, $J=7$), 2.88–2.96 (m, 4H), 3.51 (br d, 2H), 3.88 (s, 3H), 6.93 (d, 2H, $J=8.9$), 7.93 (d, 2H, $J=8.9$); ^{13}C NMR ($CDCl_3$, 100 MHz) δ 22.1, 22.3, 23.3, 23.4, 26.4, 37.5, 53.1, 55.5, 57.2, 113.8, 129.9, 130.3, 163.5, 198.5; MS (EI, 70 eV) *m*/*z* (relative intensity, %): 289 (M^+, 3); HRMS (EI, M^+) calcd for $C_{19}H_{27}NO_2$: 289.2042. Found: 289.2060.

1,3-Bis-(4-methoxy-phenyl)-2-(4-*N*-piperidinyl-butyl)-propane-1,3-dione (12). To a solution of ketone **11** (350 mg, 1.21 mmol) and TMEDA (140.6 mg, 0.18 mL, 1.21 mmol) in THF (15 mL) at 0 °C was added a 1.0 M solution of LiHMDS (3.02 mL, 3.02 mmol) dropwise. The solution was allowed to stir at rt for 0.5 h, then was cooled back to 0 °C. At this time a solution of 4-nitrophenyl 4-methoxybenzoate (990 mg, 3.63 mmol; prepared from *p*-nitrophenol and 4-methoxybenzoic acid using DIC and DMAP coupling conditions) in THF (5 mL) was added dropwise. The resulting solution was allowed to stir for 15 h at rt and 4 h at reflux (oil bath temperature of 70 °C). At this time the mixture was allowed to come to rt and quenched by the addition of H_2O (10 mL). The organic layer was isolated and washed with H_2O (3×15 mL), dried over Na_2SO_4, and concentrated under reduced pressure to afford a yellow solid. The remaining ester was removed by warming the crude mixture in 15% ethyl acetate/hexanes and filtering off the excess crystalline ester. The filtrate was concentrated under reduced pressure and purified by flash chromatography (10% TEA and 55% EtOAc in hexanes) to afford **12** as a yellow oil (227 mg, 51%): ^1H NMR ($CDCl_3$, 400 MHz) δ 1.22–1.48 (m, 4H), 1.50–1.75 (m, 6H), 2.10 (q, 2H, $J=7.5$), 2.34 (t, 2H, $J=9.8$), 2.42 (br s, 4H), 3.83 (s, 6H), 5.05 (t, 1H, $J=6.6$), 6.89 (d, 4H, $J=8.9$), 7.94 (d, 4H, $J=8.9$); ^{13}C NMR ($CDCl_3$, 100 MHz) δ 24.0, 25.3, 26.1, 26.3, 29.3, 54.3, 55.4, 57.0, 58.7, 113.9, 128.9, 128.9, 130.8, 130.8, 163.6, 194.6.

3,5-Bis-(4-methoxyphenyl)-4-(4-*N*-piperidinyl-butyl)-1-phenyl-1*H*-pyrazole (13). To a stirred solution of DMF (45 mL), THF (20 mL), and β-diketone **12** (170 mg, 0.40 mmol) was added phenylhydrazine hydrochloride (289 mg, 2.00 mmol). The solution was brought to reflux (oil bath temperature between 110 and 120 °C) for 22 h. The reaction mixture was allowed to cool to rt, and the THF was evaporated under reduced pressure. The remaining mixture was diluted with H_2O (40 mL) and extracted with EtOAc (3×40 mL). The organic layers were combined and washed with saturated LiCl (3×40 mL), saturated $NaHCO_3$ (2×40 mL), H_2O (2×40 mL), and brine (2×40 mL). The organic layer was dried over $MgSO_4$ and concentrated under reduced pressure to afford a crude brown oil. Purification by flash chromatography (10% TEA and 55% EtOAc in hexanes) afforded **13** as a reddish oil (79 mg, 40%). Compound **13** was verified by ^1H NMR and used in the next step of the reaction scheme without further characterization.

1-[4-(2-*N*-Piperidinyl-ethoxy)-phenyl]-butan-1-one (14). To a solution of PPh_3 (10.05 g, 38.31 mmol) in THF (150 mL) at 0 °C was added diisopropyl azodicarboxylate (7.5 mL, 38.31 mmol) dropwise. After stirring at 0 °C for 50 min, *N*-piperidinylethanol (5.09 mL, 38.31 mmol) was added followed 10 min later by addition of a solution of 4-hydroxy-butyrophenone (5.24 g, 31.9 mmol) in Et_3N (13.4 mL, 95.8 mmol) and THF (30 mL). The mixture was allowed to warm to rt and stirred overnight and then concentrated in vacuo. To the crude residue was added Et_2O (150 mL) and the insoluble Ph_3PO by-product removed by filtration. The filtrate was concentrated once again and the residue purified by flash chromatography (10% TEA and 25% EtOAc in hexanes) to afford an oil. This material was dissolved in Et_2O (60 mL) and acidified with HCl (4 M in dioxane, 6.3 mL). The precipitate that formed was collected by vacuum filtration and partitioned between saturated $NaHCO_3$ (35 mL) and ether (50 mL). The organic layer was washed with brine, dried over Na_2SO_4 and concentrated under reduced pressure to give **14** as pale-yellow

crystals (3.05 g, 35%). An analytically pure sample was obtained by recrystallization from hexane: mp 48–50 °C; ^{1}H NMR ($CDCl_3$, 400 MHz) δ 0.99 (t, 3H, $J=7.5$), 1.43–1.49 (m, 2H), 1.64 (quint, 4H, $J=5.9$), 1.75 (sext, 2H, $J=7.6$), 2.55 (br s, 4H), 2.87 (t, 2H, $J=5.9$), 2.90 (t, 2H, $J=7.2$), 4.19 (t, 2H, $J=6.0$), 6.93 (XX′ of AA′XX′, 2H, $J_{AX}=8.9$, $J_{XX'}=2.5$), 7.93 (AA′ of AA′XX′, 2H, $J_{AX}=9.0$, $J_{AA'}=2.5$); ^{13}C NMR δ 14.1, 18.2, 24.2, 26.0, 40.4, 55.3, 57.9, 66.3, 114.4, 130.5, 162.7, 199.2; HRMS calcd for $C_{17}H_{26}NO_2$: 276.1963. Found: 276.1964.

2-Ethyl-1-(4-methoxyphenyl)-3-[4-(2-*N*-piperidinyl-ethoxy)-phenyl]-propane-1,3-dione (15). To a THF (25 mL) solution of ketone **14** (500 mg, 1.82 mmol) and 4-nitrophenyl 4-methoxybenzoate (745.3 mg, 2.73 mmol) at 0 °C was added LiHMDS (1 M solution in hexane, 4.55 mL, 4.55 mmol) dropwise. Upon complete addition of LiHMDS the solution was allowed to warm to rt and stir overnight. The reaction mixture was concentrated to near dryness and EtOAc (35 mL) added. The crude mixture was washed sequentially with saturated $NaHCO_3$ and brine. The solvent was dried over Na_2SO_4, removed in vacuo and the resulting oil purified via flash chromatography (10% TEA and 50% EtOAc in hexanes) to give **15** as a viscous red oil (465 mg, 63%): ^{1}H NMR ($CDCl_3$, 400 MHz) δ 1.03 (t, $J=7.31$), 1.49 (br s, 2H), 1.70 (br s, 4H), 2.16 (quint, $J=7.29$ Hz, 2H), 2.63 (br s, 4H), 2.90 (br s, 2H), 3.85 (s, 3H), 4.25 (br s, 2H), 4.96 (t, $J=6.76$ Hz, 1H), 6.91 (d, $J=9.05$ Hz, 4H), 7.95 (d, $J=8.96$ Hz, 2H), 7.96 (d, $J=8.85$ Hz, 2H); ^{13}C NMR ($CDCl_3$, 125 MHz) δ 12.8, 23.1, 24.0, 25.8, 55.0, 55.4, 57.6, 59.0, 66.2, 113.9, 114.5, 116.5, 129.2, 129.3, 130.9, 131.0, 163.0, 163.7, 194.9; HRMS (EI, M^+) calcd for $C_{25}H_{31}NO_4$: 409.2253. Found: 407.2096 (M^+-2).

Acknowledgements

We are grateful for support of this research through grants from the US Army Breast Cancer Research Program (DAMD17-97-1-7076) and the National Institutes of Health (PHS 5R37 DK15556 (to J. A. K.), PHS 5R37 CA18119 (to B. S. K.), PHS T32 CA09067 (traineeship for Y. R. H.)). We thank Kathryn E. Carlson for performing binding assays and Rosanna Tedesco for help with molecular graphics. NMR spectra were obtained in the Varian Oxford Instrument Center for Excellence NMR Laboratory. Funding for this instrumentation was provided in part from the W. M. Keck Foundation and the National Science Foundation (NSF CHE 96-10502). Mass spectra were obtained on instruments supported by grants from the National Institute of General Medical Sciences (GM 27019), the National Institute of Health (RR 01575), and the National Science Foundation (PCM 8121494).

References and Notes

1. Grese, T. A.; Dodge, J. A. *Curr. Pharm. Design* **1998**, *4*, 71.
2. Brzozowski, A. M.; Pike, A. C.; Dauter, Z.; Hubbard, R. E.; Bonn, T.; Engström, O.; Öhman, L.; Greene, G. L.; Gustafsson, J.-A.; Carlquist, M. *Nature* **1997**, *389*, 753.
3. Shiau, A. K.; Barstad, D.; Loria, P. M.; Cheng, L.; Kushner, P. J.; Agard, D. A.; Greene, G. L. *Cell* **1998**, *95*, 927.
4. Darimont, B. D.; Wagner, R. L.; Apriletti, J. W.; Stallcup, M. R.; Kushner, P. J.; Baxter, J. D.; Fletterick, R. J.; Yamamoto, K. R. *Genes Develop.* **1998**, *12*, 3343.
5. Katzenellenbogen, J. A.; O'Malley, B. W.; Katzenellenbogen, B. S. *Mol. Endocrinol.* **1996**, *10*, 119.
6. McDonnell, D. P.; Clemm, D. L.; Hermann, T.; Goldman, M. E.; Pike, J. W. *Mol. Endocrinol.* **1995**, *9*, 659.
7. Paige, L. A.; Christensen, D. J.; Gron, H.; Norris, J. D.; Gottlin, E. B.; Padilla, K. M.; Chang, C.; Ballas, L. M.; Hamilton, P. T.; McDonnell, D. P.; Fowlkes, D. M. *Proc. Natl. Acad. Sci. USA* **1999**, *96*, 3999.
8. Norris, J. D.; Paige, L. A.; Christensen, D. J.; Chang, C. Y.; Huacani, M. R.; Fan, D.; Hamilton, P. T.; Fowlkes, D. M.; McDonnell, D. P. *Science* **1999**, *285*, 744.
9. Chang, C. Y.; Norris, J. D.; Gron, H.; Paige, L. A.; Hamilton, P. T.; Kenan, D. J.; Fowlkes, D.; McDonnell, D. P. *Mol. Cell Biol.* **1999**, *19*, 8226.
10. Kuiper, G.; Shughrue, P. J.; Merchenthaler, I.; Gustafsson, J. A. *Frontier Neuroendocrinol.* **1998**, *19*, 253.
11. Kuiper, G. G. J. M.; Gustafsson, J.-A. *FEBS Lett.* **1997**, *410*, 87.
12. Kuiper, G. G. J. M.; Carlsson, B.; Grandien, K.; Enmark, E.; Häggblad, J.; Nilsson, S.; Gustafsson, J. Å. *Endocrinology* **1997**, *138*, 863.
13. Fink, B. E.; Mortensen, D. S.; Stauffer, S. R.; Aron, Z. D.; Katzenellenbogen, J. A. *Chem. Biol.* **1999**, *6*, 205.
14. Stauffer, S. R.; Katzenellenbogen, J. A. *J. Combinat. Chem.* **2000**, *2*, 318.
15. Stauffer, S. R.; Coletta, C. J.; Tedesco, R.; Sun, J.; Katzenellenbogen, B. S.; Katzenellenbogen, J. A. *J. Med. Chem.* **2000**, submitted.
16. Stauffer, S. R.; Huang, Y.; Coletta, C. J.; Katzenellenbogen, J. A. *Bioorg. Med. Chem.* **2000**, *9*, 141.
17. Magarian, R. A.; Overacre, L. B.; Singh, S.; Meyer, K. L. *Curr. Med. Chem.* **1994**, *1*, 61.
18. Huang, Y.; Katzenellenbogen, J. A. *Org. Lett.* **2000**, *2*, 2833.
19. Demers, J. P.; Klaubert, D. H. *Tetrahedron Lett.* **1987**, *42*, 4933.
20. Carlson, K. E.; Choi, I.; Gee, A.; Katzenellenbogen, B. S.; Katzenellenbogen, J. A. *Biochemistry* **1997**, *36*, 14897.
21. Katzenellenbogen, J. A.; Johnson, H. J. Jr; Myers, H. N. *Biochemistry* **1973**, *12*, 4085.
22. Williams, D.; Gorski, J. *Biochemistry* **1974**, *13*, 5537.
23. McInerney, E. M.; Weis, K. E.; Sun, J.; Mosselman, S.; Katzenellenbogen, B. S. *Endocrinology* **1998**, *139*, 4513.
24. Sun, J.; Meyers, M. J.; Fink, B. E.; Rajendran, R.; Katzenellenbogen, J. A.; Katzenellenbogen, B. S. *Endocrinology* **1999**, *140*, 800.
25. Grese, T. A.; Pennington, L. D.; Sluka, J. P.; Adrian, M. D.; Cole, H. W.; Fuson, T. R.; Magee, D. E.; Phillips, D. L.; Rowley, E. R.; Shetler, P. K.; Short, L. L.; Venugopalan, M.; Yang, N. N.; Sato, M.; Glasebrook, A. L.; Bryant, H. U. *J. Med. Chem.* **1998**, *41*, 1272.